Supplementary Information for

Tailoring the mechanical properties of 3D microstructures: a deep learning and genetic algorithm inverse optimization framework

Xiao Shang[1], Zhiying Liu[1], Jiahui Zhang[1], Tianyi Lyu[1], Yu Zou[1]*

[1]Department of Materials Science and Engineering, University of Toronto, Toronto, ON, Canada, M5S 3E4
*Corresponding author. Email: mse.zou@utoronto.ca

This PDF file includes:

Figures S1 to S6
Tables S1 to S9

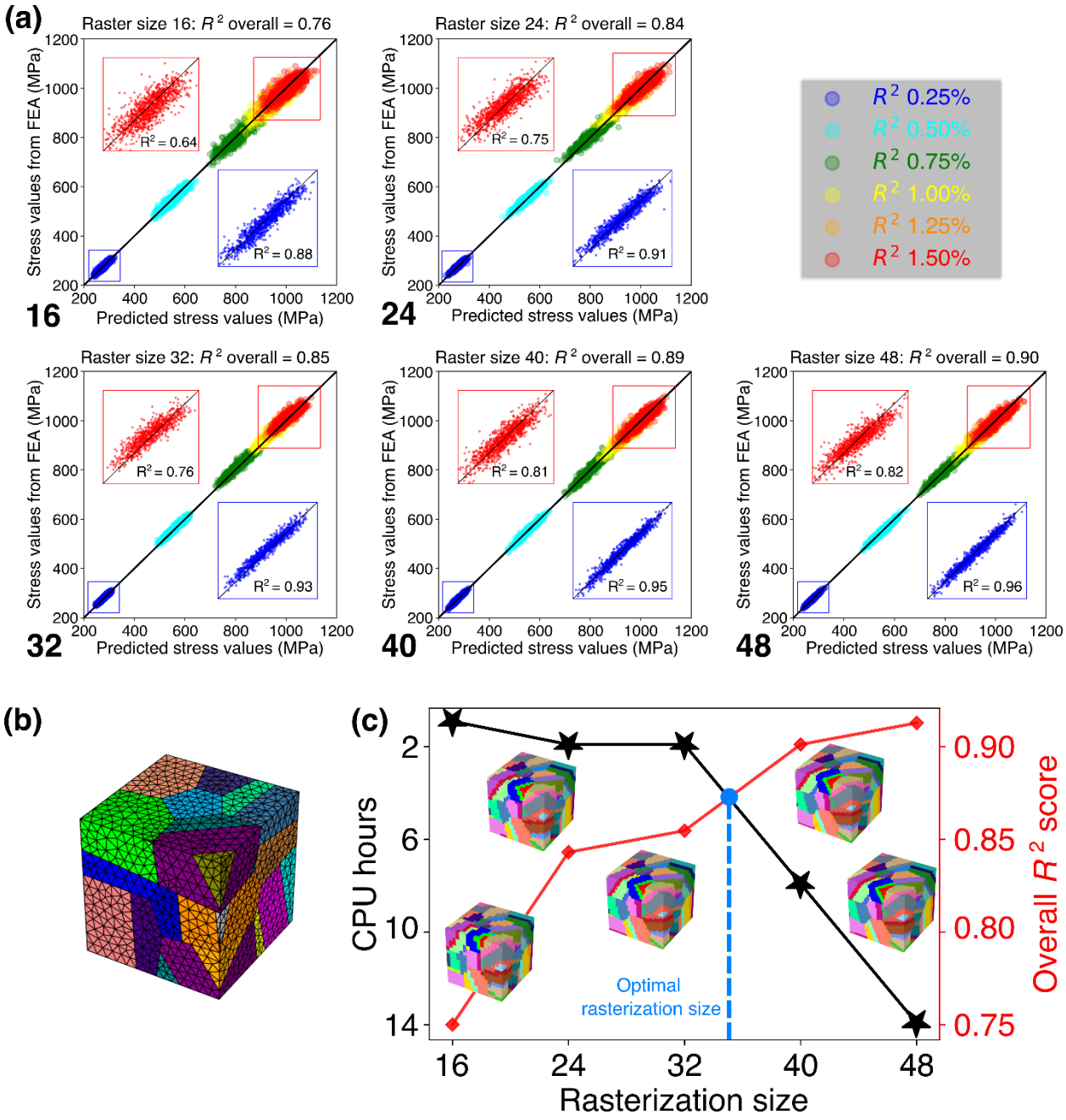

Figure S1. Parametric study on rasterization levels and 3D-CNN model performances. (**a**) Parity plots showing model performance with rasterization levels at 16, 24, 32, 40, and 48. The insets are zoomed-in views at 0.25% (blue) and 1.50% (red) strains, respectively. (**b**) A sample microstructure meshed with tetrahedral meshes used for FEA simulation. (**c**) Traded-off plot of CPU hours and overall R^2 score with changing rasterization size.

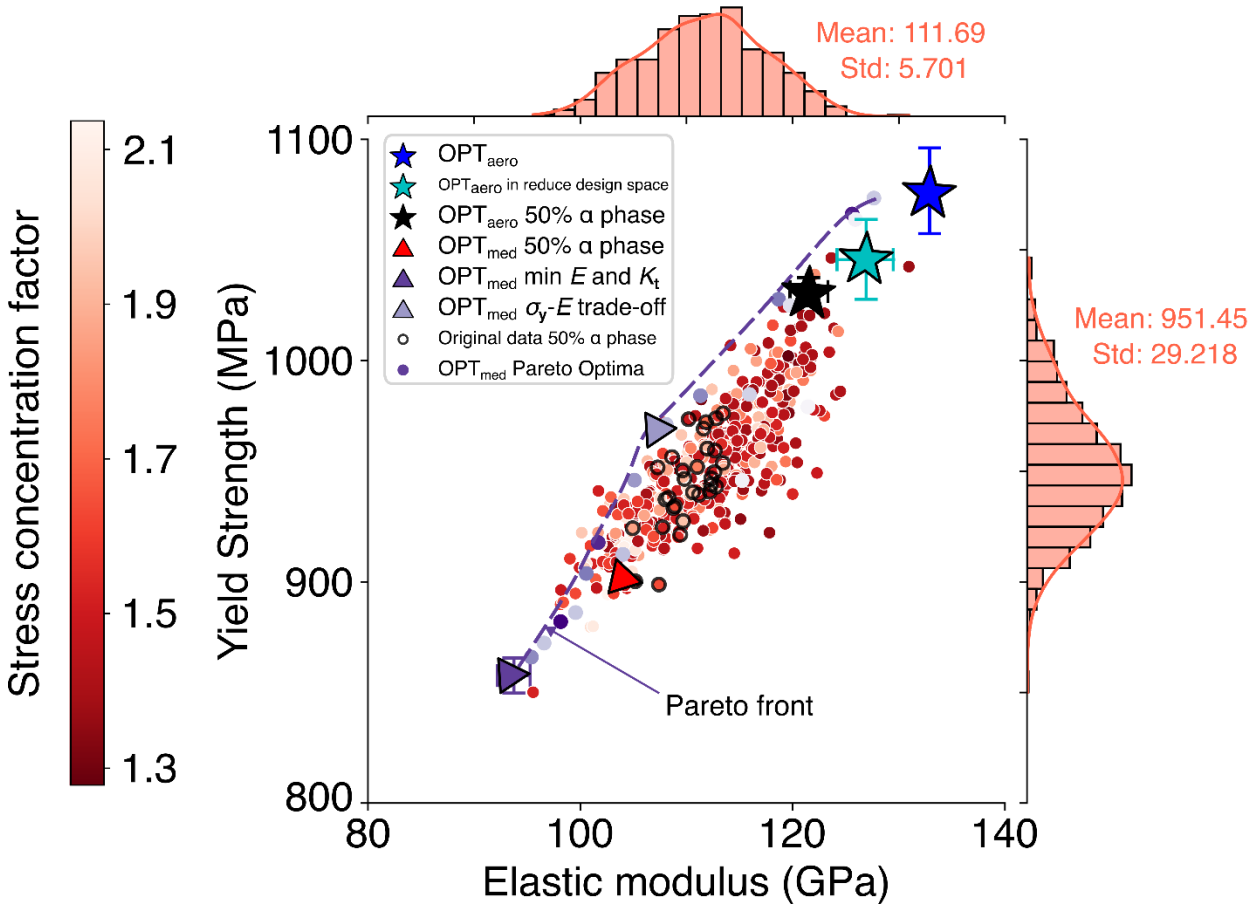

Figure S2. Optimization results and original data distributions in 2D. The red spectrum scattered points are datapoints from the original dataset, coloured by their corresponding stress concentration factor (K_t) values. The purple spectrum scattered points are the nondominated solutions identified in OPT_{med1}. Data points with 50% α phase from the original dataset are circled in black. Mechanical properties of the microstructures identified by optimizations are plotted with their means and standard deviations, except for the OPT_{med} σ_y-E trade-off case, for which the result from OPT_{med1} is shown. Distribution histograms of the elastic modulus (E) and yield strengths (σ_y) are visualized on the top and right sides of the plot, respectively.

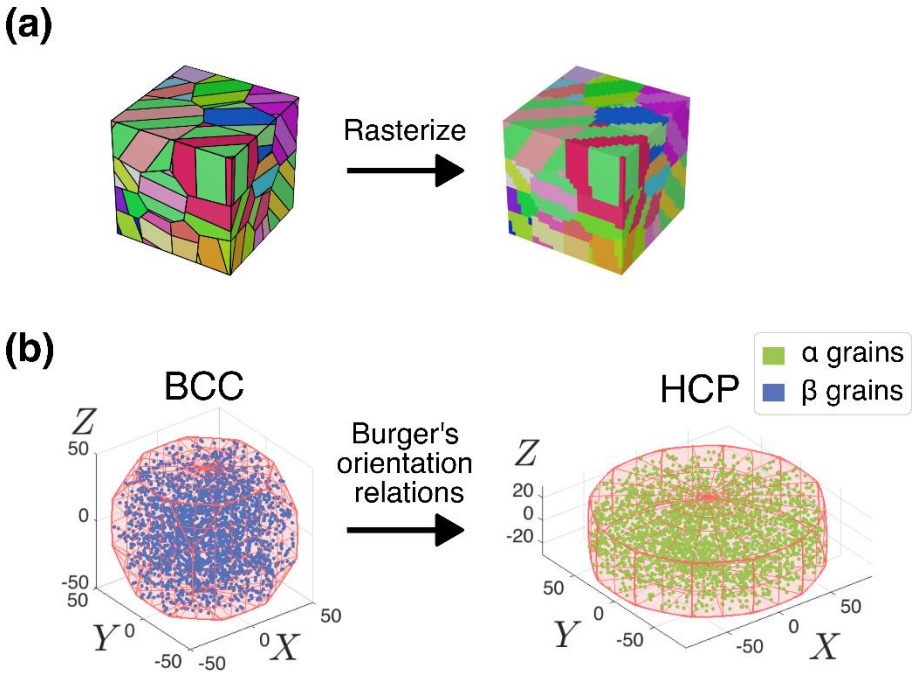

Figure S3. Microstructure preparation. (**a**) Rasterizing an artificially generated microstructure into a 32 x 32 x 32 3D image to use as deep learning model input. (**b**) Orientation distributions of the α and β grains in the dataset, plotted in their corresponding fundamental regions, respectively. The α grain orientations are calculated from the β grain orientations by enforcing the Burger's orientation relations.

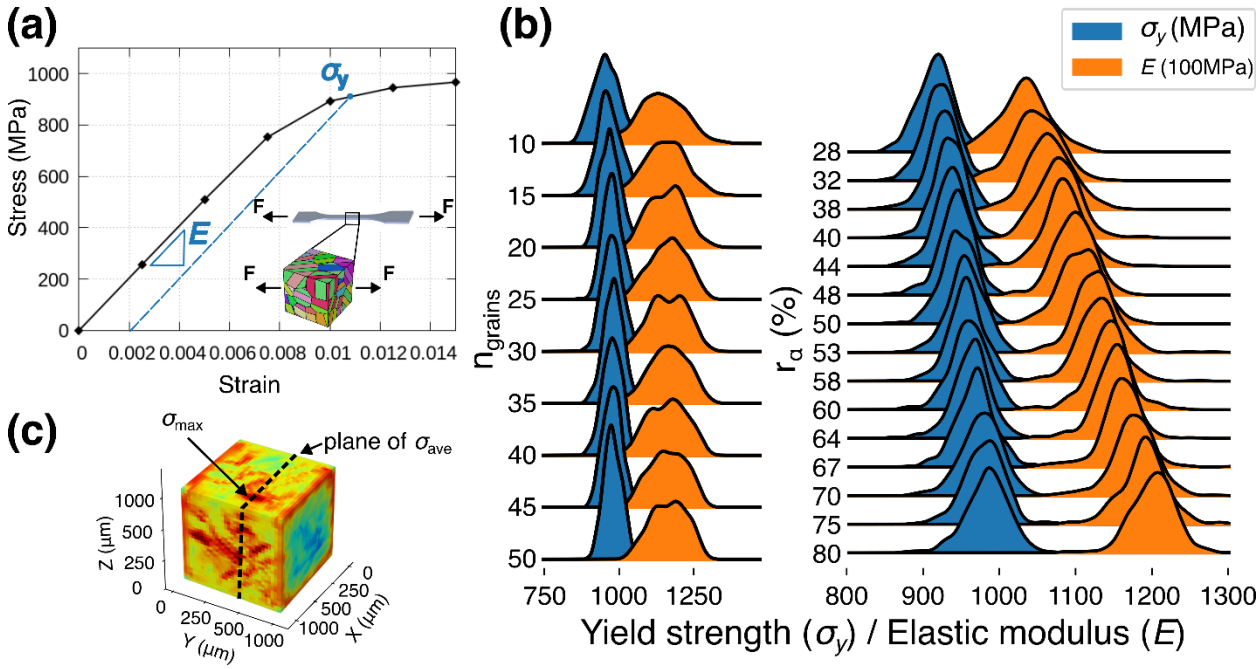

Figure S4. Mechanical responses and the distribution of σ_y and E. (**a**) A sample stress-strain curve for a 3D microstructure under uniaxial tension with 0.2% offset yield strength (σ_y) and elastic modulus (E) marked. The inset displays a tensile test coupon under uniaxial loading and how a 3D microstructure represents its cross section in this work. (**b**) Distributions of σ_y and E for nearly 6,000 data in the dataset. The left shows the distributions' change with number of prior β grains (n_{grains}), while the right shows their change with α phase volume fraction (r_α). (**c**) Sample von Mises stress field with σ_{max} and σ_{ave} plane marked.

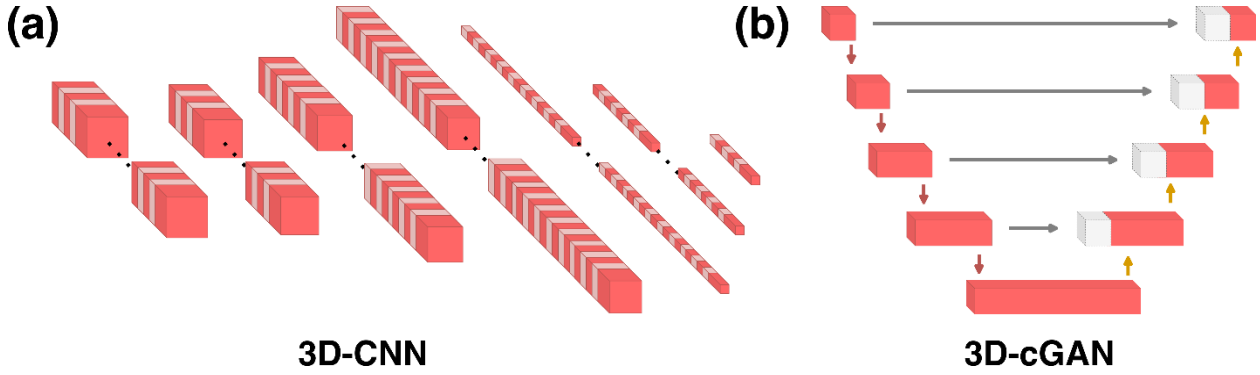

Figure S5. Schematic illustration of proposed 3D deep learning model architectures. (**a**) 3D convolutional neural network (3D-CNN) model. (**b**) 3D conditional generative adversarial network (3D-cGAN) model.

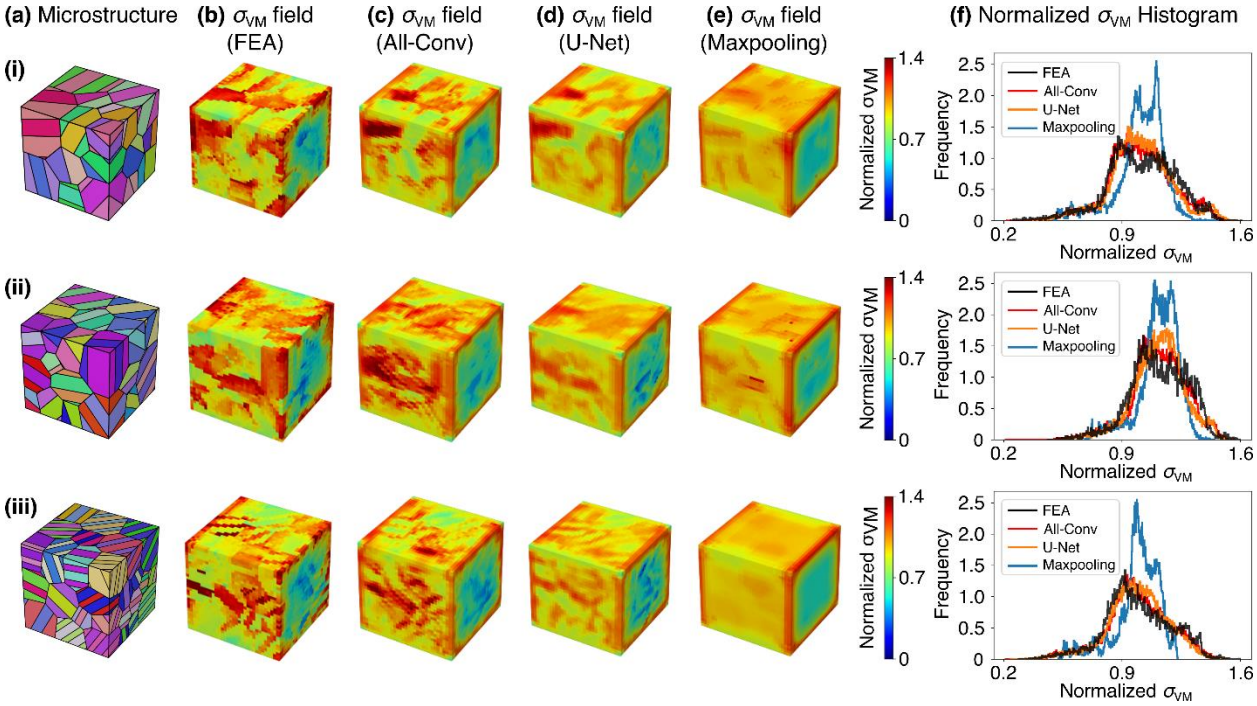

Figure S6. Generator performance comparison on three randomly selected microstructures. (**a**) Selected microstructures. (**b**) – (**e**) von Mises stress distribution fields by FEA calculation, all-convolutional generator prediction, original U-Net generator prediction, all-max-pooling generator prediction, respectively. (**f**) von Mises stress histograms of stress distributions from FEA calculation and various generators prediction.

Table S1. Mean absolute errors and mean absolute percentage errors of the 3D-CNN model predictions for each by stress point and for the elastic and plastic regimes.

Strains (%)	**0.25**	**0.50**	**0.75**	**1.00**	**1.25**	**1.50**
Mean (MPa)	280.13	558.66	815.39	944.55	989.20	1009.35
Mean absolute error (MAE, MPa)	3.011	6.073	8.914	10.933	11.698	11.880
Mean absolute percentage error (MAPE, %)	1.075	1.087	1.093	1.157	1.183	1.177
MAPE by regime (%)		**Elastic regime**			**Plastic regime**	
		1.085			1.172	

Table S2. Detailed results of various optimization tasks in inverse exploration.

	σ_y (MPa)	E (GPa)	K_t	α phase fraction
OPT_{aero1}	1054.8	132.2	1.24	0.924
OPT_{aero2}	1084.4	132.8	1.30	0.864
OPT_{aero3}	1090.5	133.7	1.34	0.828
Mean	1076.56	132.89	1.29	0.872
Std	22.418	4.148	0.004	0.077
OPT_{aero1} without K_t	1098.5	138.2	-	0.930
OPT_{aero2} without K_t	1105.1	135.1	-	0.923
OPT_{aero3} without K_t	1116.6	139.1	-	0.913
Mean	1106.71	137.45	-	0.922
Std	9.178	2.134	-	0.009
OPT_{aero1}, 50% α phase	1024.9	119.7	1.41	0.500
OPT_{aero2}, 50% α phase	1030.5	121.1	1.39	0.500
OPT_{aero3}, 50% α phase	1001.1	116.4	1.33	0.500
Mean	1018.83	119.09	1.38	0.500
Std	15.569	2.425	0.036	-
OPT_{med1} min E and K_t	854.7	92.7	1.55	0.321
OPT_{med2} min E and K_t	850.3	92.6	1.54	0.292
OPT_{med3} min E and K_t	866.0	95.4	1.48	0.319
Mean	857.00	93.57	1.52	0.311
Std	8.099	1.589	0.038	0.016
OPT_{med1} σ_y-E trade-off	971.1	108.1	1.40	0.323
OPT_{med2} σ_y-E trade-off	960.0	108.8	1.55	0.287
OPT_{med3} σ_y-E trade-off	953.5	106.0	1.59	0.324
Mean	961.53	107.63	1.513	0.311
Std	7.267	1.190	0.082	0.017
OPT_{med1}, 50% α phase	901.8	104	1.35	0.500
OPT_{med2}, 50% α phase	904.2	103	1.37	0.500
OPT_{med3}, 50% α phase	897.7	105.4	1.29	0.500
Mean	901.2333	104.1333	1.336667	0.500
Std	3.286842	1.205543	0.041633	-

Table S3. Detailed results of OPT_{areo} in the inverse exploration in a reduced design space with α phase fraction of 28%-80%.

	σ_y (MPa)	E (GPa)	K_t	α phase fraction
OPT_{aero1}	1066.4	129.6	1.29	0.779
OPT_{aero2}	1030.7	124.2	1.27	0.731
OPT_{aero3}	1039.7	127.1	1.30	0.773
Mean	1045.61	126.94	1.289	0.761
Std	18.558	2.723	0.018	0.026

Table S4. Statistics of σ_y, E, and K_t of the microstructures with 25 prior-β grains in the original dataset.

***α* phase ratio**		***28%-80%***			***50% only***	
Properties	σ_y (MPa)	E (GPa)	K_t	σ_y (MPa)	E (GPa)	K_t
Count	473	473	473	30	30	30
Mean	951.45	111.69	1.61	944.63	110.24	1.65
Std	29.218	5.701	0.212	19.495	2.350	0.195
Min	850.1	95.6	1.28	898.79	104.95	1.34
25%	931.5	107.8	1.45	934.99	108.69	1.49
50%	949.4	111.9	1.52	945.22	110.42	1.61
75%	969.0	115.5	1.81	955.73	112.30	1.79
Max	1046.4	130.9	2.14	976.18	113.48	2.07
Microstructure with maximum σ_y and E	1046.4	123.64	1.40	976.18	113.48	1.60
Microstructure with minimum E	850.1	95.6	1.52	924.25	104.95	1.86

Table S5. Material elastic constants used in FEA simulation.

Phases	C_{11} (GPa)	C_{12} (GPa)	C_{13} (GPa)	C_{44} (Gpa)
a	169.66	88.66	61.66	42.50
b	133.10	95.10	-	42.70

Table S6. Initial Slip strengths and plasticity parameters used for both α and β phases in FEA simulation. The parameters shaded in light orange are assumed parameters.

$g_{0,b}$ (MPa)	$g_{0,b}$ (MPa)	$g_{0,p}$ (MPa)	$g_{0,p}$ (MPa)	h_0 (MPa)	g_{s0} (MPa)	m	m'	$\dot{\gamma}_0\ (s^{-1})$	$\dot{\gamma}_{s0}\ (s^{-1})$
390	468	390	663	190	530	0.01	0.01	1.0	$5x10^{10}$

Table S7. 3D-CNN model architecture.

Layer #	Layer type*	Output shape
1	Input layer	32x32x32x4
2	Conv3D+BatchNormalization	30x30x30x32
3	Conv3D+BatchNormalization	28x28x28x32
4	Conv3D+BatchNormalization	26x26x26x64
5	Conv3D+BatchNormalization+GlobalAveragePooling3D	128
6	Dense+Dropout	64
7	Output layer	6

*Layer type use the abbreviate terminology in TensorFlow.

Table S8. 3D-cGAN model architecture.

Model type	Layer #	Layer type*	Output shape	Pre-trained	# of trainable parameters
Generator (All convolutional)	1	Input layer	32x32x32x4	-	859,265 with transfer learning / 1,167,361 without transfer learning
	2	Conv3D+BatchNormalization	30x30x30x32	Y	
	3	Conv3D+BatchNormalization	28x28x28x32	Y	
	4	Conv3D+BatchNormalization	26x26x26x64	Y	
	5	Conv3D+BatchNormalization	24x24x24x128	Y	
	6	Conv3DTanspose+ BatchNormalization	26x26x26x128	Y	
	7	Conv3DTanspose+ BatchNormalization	28x28x28x64	N	
	8	Conv3DTanspose+ BatchNormalization	30x30x30x32	N	
	9	Output layer	32x32x32x1	N	
Discriminator	1	Input layer	32x32x32x4 + 32x32x32x1	-	
	2	Concatenate layer	32x32x32x5		
	3	Conv3D	30x30x30x32	-	
	4	Conv3D+BatchNormalization	28x28x28x32	-	
	5	Conv3D+BatchNormalization	26x26x26x64	-	
	6	ZeroPadding3D	28x28x28x64	-	
	7	Conv3D+BatchNormalization	26x26x26x128		
	8	ZeroPadding3D	28x28x28x128		
	9	Conv3D	26x26x26x1		

*Layer type use the abbreviate terminology in TensorFlow.

Table S9. Architectures of 3D-cGAN model comparable generators.

Model type	Layer #	Layer type*	Output shape	# of trainable parameters	Transfer learning
Original U-Net	1	Input layer	32x32x32x4	950,401	No
	2	Conv3D+Maxpooling	30x30x30x32		
	3	Conv3D+Maxpooling	28x28x28x32		
	4	Conv3D+ Maxpooling	26x26x26x64		
	5	Conv3D+ Maxpooling	24x24x24x128		
	6	Conv3DTanspose+ BatchNormalization	26x26x26x128		
	7	Conv3DTanspose+ BatchNormalization	28x28x28x64		
	8	Conv3DTanspose+ BatchNormalization	30x30x30x32		
	9	Output layer	32x32x32x1		
All-max-pooling architecture	1	Input layer	32x32x32x4	302,125	No
	2	Maxpooling	30x30x30x32		
	3	Maxpooling	28x28x28x32		
	4	Maxpooling	26x26x26x64		
	5	Maxpooling	24x24x24x128		
	6	Conv3DTanspose+ BatchNormalization	26x26x26x128		
	7	Conv3DTanspose+ BatchNormalization	28x28x28x64		
	8	Conv3DTanspose+ BatchNormalization	30x30x30x32		
	9	Output layer	32x32x32x1		

*Layer type use the abbreviate terminology in TensorFlow.